

# ANALYSIS OF CLOUD DISTRIBUTION EFFECT ON DAYLIGHTING IN URBAN ENVIRONMENT

**Thibaut Vermeulen, Luis Merino, Benoit Beckers**

*Avenues, Urban Systems Engineering Department,*

*Compiègne University of Technology, France*

*thibaut.vermeulen@etu.utc.fr, merinolu@utc.fr, benoit.beckers@utc.fr*

**Keywords:** daylighting, cloud distribution, urban coefficient of reflection, radiosity method.

## Abstract

The optimization of natural light is an important criterion for sustainable building in order to reduce the energy consumption due to artificial illumination. This article tackles this problem by using a simple urban case to simulate natural lighting. The main goal is to identify those parameters affecting interior daylighting.

The case studied consists in a room oriented north, facing an infinite-wall across a street under an isotropic sky corrected with monthly cloud distribution of two locations at the same latitude. The computation was made using the radiosity method to determine the illuminance inside the room taking into account the sky diffuse radiation and all surfaces reflections. Results of daylighting inside the room were calculated for two values of the exterior wall coefficient of reflection. Preliminary results show that the urban color tend to influence greatly the inner illuminance, and slightly the daily number of hours with a standard visual comfort.

## 1. Introduction

Since the ambition of building more sustainable cities becomes a major preoccupation, daylighting represents an important parameter in constructions to increase winter and summer comfort while decreasing energy consumption. The bioclimatic fundamentals concerning solar energy are well known for a single building in an open space, and some work of modeling was undertaken using sky models to consider the climate particularities [18]. In an urban environment, the access to light is less obvious because every building can be a mask and a reflector, preventing surrounding buildings to benefit from solar and sky radiation, and retransmitting some of the received natural energy depending on its coefficient of reflection (*i.e.* the ratio of incoming energy reflected by a surface). From this observation, the problem is to find optima on received energy and daylighting by modifying the urban specifications (orientation, geometry, coefficient of reflection) to fit with the local natural resources in order to receive adequate daylighting for interior spaces, or maximize the exterior energy on PV panels [12].

This paper describes a simulation of radiative exchanges in a room taking into account the urban scene, considering direct and diffuse radiations and their reflections on the different surfaces. The sun and sky irradiances are simulated with the clear sky model from Liu & Jordan as cited by Campbell [2, 11, 1] weighted with measured data from Ottawa (Ca), and Limoges (Fr) [15]. In the first part, the parameters of the model and of the computation are presented. In a second part, some results of simulations are given in terms of illuminance with a comparison for two values of the exterior coefficient of reflection for the two city locations.

## 2. Settings of the simulation model

### 2.1 A very simple urban configuration

The case studied in this paper is an office room with a single hole (or window with a transmittance of 1) oriented north, facing a wall, across a street, which reflects some of the solar energy coming from the south as well as the energy coming from the sky vault.

The simulations were computed between 8AM and 4PM, corresponding to regular working hours. It allows, whatever the day on which calculation is made, to stay in the daytime, with a sun located in the southern half of the sky vault (for the latitude of Ottawa and Limoges, 45,5°N). The interior of the room never receives direct radiation from the sun. The flux of energy that reaches the room from the exterior has three components:

- the reflection of the solar direct radiation on the wall across the street (depending on solar height and azimuth, coefficient of reflection of the wall, and cloud distribution),
- the sky vault directly seen from the interior surfaces (depending on solar height and cloud distribution) and
- the reflection of the sky vault diffuse radiation on the wall across the street (depending on solar height, coefficient of reflection of the exterior wall and cloud distribution).

The simulation case is a room of 24m<sup>2</sup> with a window occupying the upper half of the northern wall (Figure 1). The length of the street, and thus the width of the wall across the street, are considered infinite.

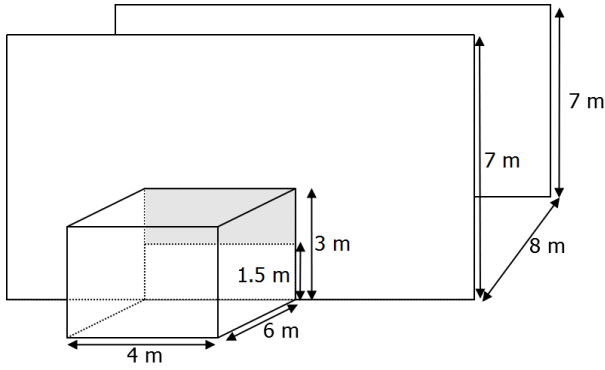


Figure 1. Simulation case

In all following examples, the coefficients of reflection of the surfaces inside the room are set to 0,4 for the floor (grey floor), and 0,7 for the walls and the ceiling (matte white paint). The street floor and the wall in the extension of the room are black (coefficient of reflection of 0).

## 2.2 Description of the sky model

### 2.2.1. The model

In the present work, we have chosen a simple model which assumes that the direct and diffuse components of the solar radiation at ground level are a function of the distance that solar beam travels through the atmosphere which is characterized by the transmittance of the atmosphere, the solar extraterrestrial radiation, the orientation and coordinates of the surface. The direct atmospheric transmittance ( $\tau_D$ ) to solar radiation of the atmosphere is the fraction of the radiation incident at the top of the atmosphere or extraterrestrial radiation that reaches the ground surface along the vertical (or zenith) path, which is the shortest path length between outer space and the surface. The direct atmospheric transmittance ( $\tau_D$ ) ranges from 0,6 to 0,75 for clear-day scenarios [2, 11]. If we assume isotropic sky and that the slant path is  $m$  times the zenith path, then the transmittance along the slant path will be  $\tau_D^m$  [7], The direct irradiance that reaches the ground surface along a slant is [2] [7]:

$$G_{tilted} = G_{sc} \tau_D^m \cos \theta \quad (1)$$

Where  $\theta$  is the incident angle i.e. the angle between the solar beam and the normal of the surface [4],  $G_{sc}$  is the extraterrestrial radiation, and  $m$  is the air mass:

$$m = \frac{e^{-\frac{z}{8200}}}{\cos \theta_z} \quad (2)$$

The diffuse radiation on a horizontal surface for clear days can be calculated by [2]:

$$G_d = 0,3(1 - \tau_D^m) G_{sc} \cos \theta_z \quad (3)$$

Where  $\theta_z$  is the solar zenith angle i.e. the angle between the beam and the zenith. The value of  $\tau_D$  was set at 0,7 [13] and the extraterrestrial radiation at  $G_{sc}=1367 \text{ W/m}^2$  [4]. The direct and diffuse component expressions were built for clear sky conditions but in practice atmospheric effects affect the intensity of solar radiation because of clouds and other aspects (temperature, pollution, etc.). Due to the extremely variable cloudiness degree, the intensities of direct and diffuse radiation under normal sky conditions will also be highly variable and their values at any instant are impossible to predict. Therefore, any attempt to establish a relationship to estimate the solar radiation and its components during cloudy days must involve statistical approaches which can be obtained from experimental data covering a sufficiently long period of time [13].

### 2.2.2. The data

The lack of data on solar radiation records worldwide [16] is one of the main problems when dealing with solar radiation modeling and forecast in a particular location. Besides, nature of data and level of aggregation is different from place to place [13]. These restrictions are an impediment when trying to obtain a generic model with high global applicability for solar energy evaluation and long-term analysis. Nowadays, several integrated information systems (database completed by a software) exist [3], with different spatial and time resolutions, input databases, covered area, parameters available and computational methods of interpolation [5]. In this work we have chosen two locations for the simulation process: Limoges and Ottawa, due to a direct availability of the real measurements in the World Radiation Data Center. An initial effort was made to reduce the error of data inputs in the simulation process by using monthly averaged insolation incident on a horizontal surface ( $\text{kWh/m}^2/\text{day}$ ); obtained from the NASA Surface meteorology and Solar Energy [15]. This is an online database which provides free solar radiation data. In this case, we used the “data tables for a particular

		Jan	Feb	Mar	Apr	May	Jun	Jul	Aug	Sep	Oct	Nov	Dec
Direct radiation	Liu & Jordan	1	1	1	1	1	1	1	1	1	1	1	1
	Limoges	0,53	0,52	0,48	0,45	0,42	0,44	0,49	0,53	0,52	0,49	0,49	0,53
	Ottawa	0,69	0,68	0,58	0,53	0,42	0,44	0,47	0,48	0,50	0,52	0,52	0,66
Diffuse radiation	Liu & Jordan	1	1	1	1	1	1	1	1	1	1	1	1
	Limoges	1,46	1,61	2,00	1,86	2,24	2,24	2,20	2,12	1,97	1,57	1,45	1,38
	Ottawa	1,59	1,77	2,03	1,84	2,17	2,18	2,14	2,09	1,89	1,56	1,42	1,48

Table 1. Coefficients for beam and diffuse radiation each month on Limoges and Ottawa locations

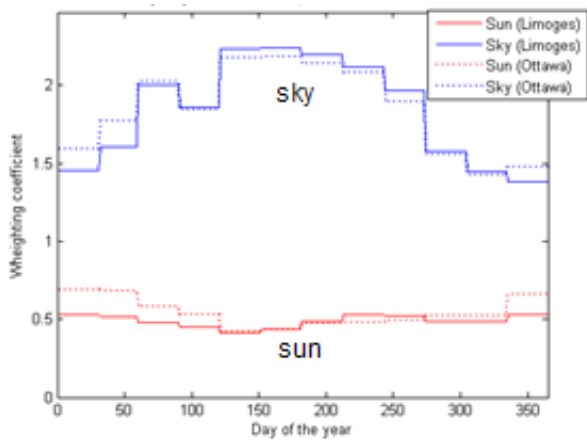


Figure 2. Weights compared to Liu & Jordan clear sky

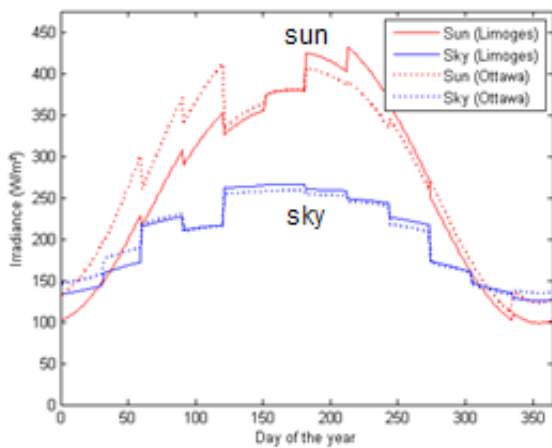


Figure 3. Irradiance from sun and sky on a horizontal plane at noon using the weighted sky model

location". The direct component projected onto a horizontal surface was calculated by subtracting the diffuse part from the global radiation.

The weighted theoretical values are presented in Table 1. Figure 2 gives a representation of the sun and sky coefficients and Figure 3 represents the application of the coefficient to weight the model, with results given on a horizontal plane. The coefficients reflect an insolation slightly more important in Ottawa than in Limoges for winter months, and the contrary in the summer period.

## 2.3 Computing hypotheses and method

**2.3.1 Simulation hypotheses.** Numerous methods exist to model the radiative exchanges, each having advantages and drawbacks. Computing the irradiance, even for a simple scene, can become quickly very time and/or memory consuming, depending on the method used [6]. In our simulation, some hypotheses have been taken to simplify the model and to reduce the complexity of the computation:

- the room has to be meshed, implying that the values of flux received or emitted are equal for small surfaces,
- the surfaces are considered as lambertian diffuse emitters, which means that the reflection of flux by any

of the surfaces is independent of the direction of emission,

- the surfaces are colored with grey levels: the reflections is the same for all the radiative spectrum and
- the emission of radiative flux from the interior to the exterior wall and sky is negligible.

**2.3.2. Computing with the radiosity method.** The simulation have been realized using the radiosity method [6]. This method, well known in the field of computer graphics, is very effective to calculate the radiosity (*i.e.* the radiative flux emitted by  $m^2$  of surface) on ideal diffuse surfaces. It consists in resolving a matrix system where each element of surface  $P_i$  is linked to the other elements by the relation:

$$B_i = E_i + \rho_i \sum_{j=1}^N F_{ij} B_j \quad (4)$$

Where  $B_i$  is the radiosity of element  $P_i$ ,  $E_i$  the flux initially emitted by surface  $P_i$ ,  $\rho_i$  the coefficient of reflection of surface  $P_i$  and  $F_{ij}$  the view factor between surfaces  $P_i$  and  $P_j$  representing the fraction of energy leaving surface  $P_i$  that reaches surface  $j$ . The view factor is defined by:

$$F_{ij} = \int_{x \in P_i} \int_{y \in P_j} \frac{\cos \theta \cos \theta'}{\pi r^2} V(x, y) dy dx \quad (5)$$

Where  $x$  (resp.  $y$ ) is a point of  $P_i$  (resp.  $P_j$ ),  $\theta$  (resp.  $\theta'$ ) is the angle between the line  $xy$  and the normal to the patch  $P_i$  at point  $x$  (resp.  $P_j$  at point  $y$ ),  $r$  is the distance between  $x$  and  $y$ , and  $V(x, y)$  is a function of visibility which value is 1 if  $x$  sees  $y$ , and 0 if  $x$  and  $y$  do not see each other.

The computing is carried out in successive steps: first, the view factors between the interior surfaces and the exterior sources (sky vault and reflector wall) are calculated to obtain the energy from the exterior that reaches the interior. Then the view factors inside the room are calculated analytically for inner reflections using combinations of known formulas [6, 8]. Once the view factors are calculated, the equation of radiosity is solved directly with a matrix inversion.

The following results are computed on fictitious sensors which are considered as differential areas facing upward. View factors between the sensors and the scene are calculated analytically for each sensor position.

## 3. Results

In this part, all results are expressed in terms of illuminance (lux), the amount of visible light received by a surface. The daylight efficacy considered to convert energy flux to luminous flux has been set to  $110 \text{ lm/w}$  ( $1 \text{ lux} = 1 \text{ lm/m}^2$ ) corresponding to average conditions for global illumination [17, 10].

The illuminance is the subject of numerous regulations or at least advices in different countries to ensure an adequate visibility required for the different conditions of work. Hence, an illuminance of 400 to 500 lux is usually recommended for an office work. We consider in this paper 400 lux as a minimum value below which the use of artificial lighting might be necessary.

### 3.1 Relative importance of the different sources of radiation

Daylight reaching the room has three components: sun reflecting on the exterior wall, sky vault reflecting on the exterior wall, and sky directly seen from the surface of the sensor. Therefore, it is possible to identify *in fine* the components of the energy received by a sensor:

- the sky directly seen from the sensor, depending on the view factor from the sensor to the sky,
- the wall across the street which reflects some of the sun and sky energy, depending on the view factor from the sensor to the wall and
- the reflection from inner surfaces.

The sum of this three components gives the final illuminance of the sensor. Figure 4 shows the illuminance along the day on December 21st in the location of Limoges for three sensors at different distances from the window, in the middle of the width of the room, at 1m high (work plan height). In these examples, the coefficient of reflection of the exterior wall was set at 0,4 (raw grey concrete) [9].

The influence of the inner reflections of the room surfaces in the illuminance is rather constant considering the three sensors. The component depending on the wall reflection exists in every case, and increases with the proximity of the window because it increases as well the view factor to the wall. Finally, sky visibility appears to be the crucial factor of illuminance, varying between 0 and several thousands of lux between the three sensors.

These results are just a representation of how the importance of the different sources can vary only for the current geometric proportions. To improve the amount of light at a spot of the room, the scene can then be modified in two ways:

- improving the view factors to the most important sources: a higher and closer wall would for example increase the view factor to the wall and diminish the view factor to the sky, changing the relative importance of both sources and
- improving the flux emitted by the different reflexive surfaces by changing their coefficient of reflection (concerns only the surfaces into the room and the exterior wall).

### 3.2 Evaluation of the effect of the coefficient of reflection of the exterior wall

In an urban context, the coefficient of reflection is a parameter relatively easy to modify because it does not require heavy modifications of the structure of the buildings.

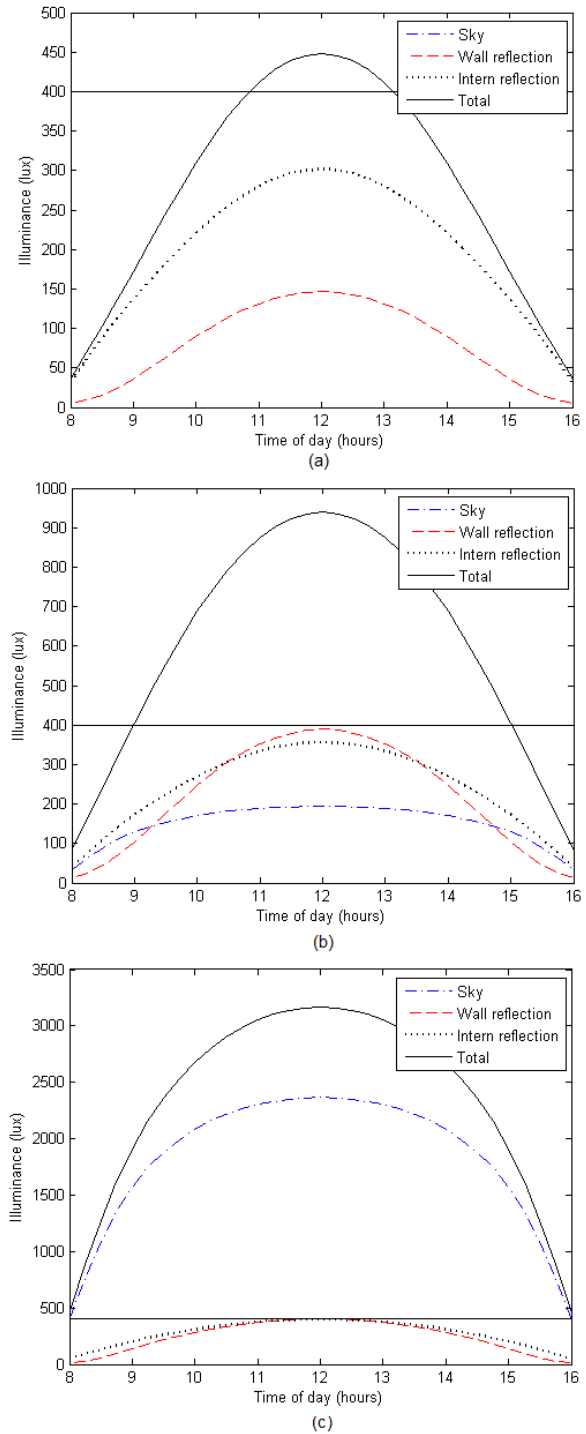


Figure 4. Components of the flux received on sensors  
 (a) at 5m from the window  
 (b) at 3m from the window  
 (c) at 1m from the window

In this part, we evaluate the effect of a repainting of the exterior wall, changing its coefficient of reflection from 0,4 (raw grey concrete), to 0,7 (white stone cladding or clear paint, for example) [9]. All other characteristics of the scene remain the same.

The illuminance is computed on sensors distributed in a grid on the section of the room located in the middle of the width, using the sun and sky weightings of Limoges and Ottawa on December 21th, from 8AM to 4PM, assuming that this date represents the worst conditions of natural light. All the sensors are horizontal and only receive light from above. The results on Figure 5 are presented as a number of hours between 8h and 16h with an illuminance minimum of 400 lux.

Some results are given in Table 2 for a sensor at 1 meter from the back wall of the room, 1 meter high (this sensor does not see directly the sky vault). For the two cities, increasing the coefficient of reflection of the reflector wall induces a slight improvement of the daytime with enough daylight (between 1h30 and 2h15). However, increasing the coefficient of reflection increases the average illuminance for more than 30% in both city cases, meaning that the daylit hours are much brighter (Table 3). It is finally possible to notice a difference around 12-13% between the two locations in terms of average illuminance.

	$\rho=0,4$	$\rho=0,7$	$\Delta(\%)$
Limoges	279	416	32,9%
Ottawa	319	480	33,5%
$\Delta(\%)$	12,5%	13,3%	

Table 2. Average illuminance on sensor (lux)

	$\rho=0,4$	$\rho=0,7$	$\Delta$
Limoges	2h17	4h32	2h15
Ottawa	3h21	4h58	1h37
$\Delta$	1h04	26 min	

Table 3. Time above 400 lux on sensor

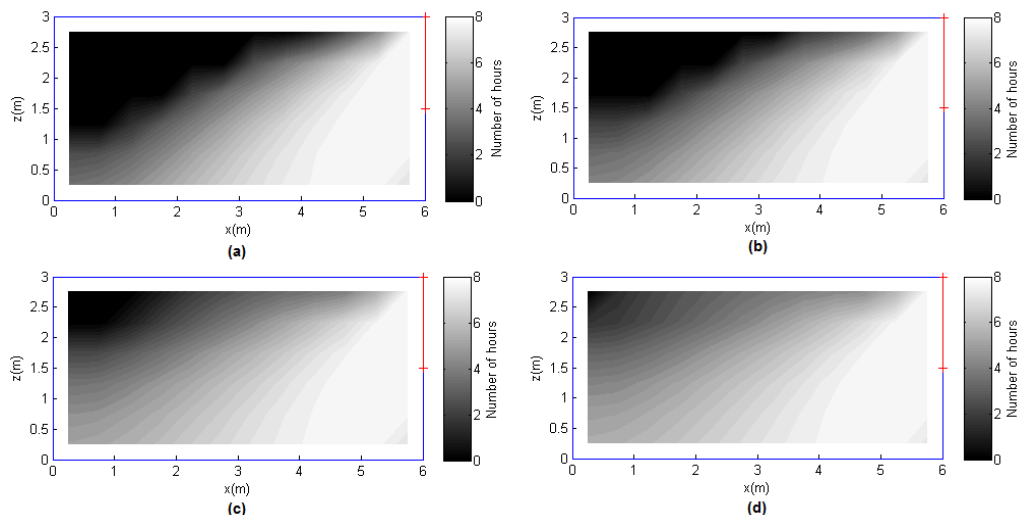


Figure 5. Number of hours above 400 lux on December 21th

- (a) Limoges,  $\rho=0,4$
- (b) Ottawa,  $\rho=0,4$
- (c) Limoges,  $\rho=0,7$
- (d) Ottawa,  $\rho=0,7$

## 4. Conclusion

In this paper, a simple simulation of an urban configuration has been presented. The daylighting have been computed in the most unfavorable day of the year for two cities at the same latitude but with different cloud distributions along the year. The model uses measured meteorological data to take into account the local cloud distribution by leveling the direct and diffuse component of the clear sky model of Liu & Jordan as cited by Campbell [2]. The average sky modeled in this study shows that Ottawa has a clearer sky in winter than Limoges, whereas Limoges receives more radiative power in summer. High values of the exterior wall coefficient of reflection, which is one of the urban parameter that influences interior daylighting, appears to improve the average illuminance on a interior spot which cannot see directly neither the sun nor the sky vault, but changes only slightly the number of hours with sufficient daylighting. Same results computed for summer (June and July) show the same trend of the daytime with enough light, but a lower relative increase of the average illuminance (which is anyway more important than in winter).

## 5. Perspectives

To go further, the other parameters of the urban environment could be modified to reach local optima, such as the height of the buildings, the width of the street, or the room specifications (geometry, coefficients of reflection).

Besides, the differences on simulation results could be analyzed by using other meteorological databases like Meteonorm [14]. The comparison between data obtained from NASA and Meteonorm gives a difference ranging from 6% to 20% in monthly values.

## References

- [1] B. Beckers and P. Beckers. (2011, Feb.) Calcul du rayonnement solaire atténué par l'atmosphère. [Online]. [www.heliodon.net](http://www.heliodon.net)
- [2] G. Campbell and J. Norman, *An Introduction to Environmental Biophysics*. New York: Springer, 1998.
- [3] S. Cross and L. Wald, "Survey of the main databases providing solar radiation data at the ground level," in *23rd EARSel Annual Symposium Remote sensing in transition*, Belgium, 2003.
- [4] J.A. Duffie and W.A. Beckman, *Solar Engineering of Thermal Processes*, 3rd ed.: John Wiley & Sons, Inc, 2006.
- [5] D. Dumortier and ENTPE, "Description of solar resource products summary of benchmarking results examples of use," MESOR project, 2009.
- [6] C. Puech F. X. Sillion, *Radiosity & Global illumination*.: Morgan Kaufmann Publishers, Inc, 1994.
- [7] D.M. Gates, *Biophysical Ecology*, 1st ed. Mineola, New York: Dover Publications, 2003.
- [8] J.R. Howell. (2001) A catalog Radiation Heat Transfer Configuration Factors, 2nd Edition. [Online]. <http://www.me.utexas.edu/~howell/index.html>
- [9] R. Levinson and H. Akbari, "Effects of composition and exposure on the solar reflectance of portland cement concrete," *Cement and Concrete Research*, vol. 32, no. 2002, pp. 1679 – 1698, 2002.
- [10] P.J. Littlefair, "Measurements of the luminous efficacy of daylight," *Lighting Research and Technology*, vol. 20, no. 4, pp. 177-188, 1988.
- [11] B.Y.H. Liu and R.C. Jordan, "The interrelationship and characteristics distribution of direct, diffuse and total solar radiation," *Solar Energy*, vol. 4, no. 3, pp. 1-19, 1960.
- [12] J. Mardaljevic and M. Rylatt, "Irradiation mapping of complex urban environments: an image-based approach," *Energy and Buildings*, vol. 35, pp. 27-35, 2003.
- [13] L. Merino, E. Antaluca, B. Akinoglu, and B. Beckers, "Solar energy inputs estimation for urban scales applications," in *SSB*, 2010.
- [14] METEOTEST, METEONORM Version 6.x, 2010.
- [15] NASA. (2011, Jan.) NASA Surface meteorology and Solar Energy. [Online]. <http://eosweb.larc.nasa.gov/cgi-bin/sse/register.cgi>
- [16] J. Page, M. Albuisson, and L. Wald, "The European solar radiation atlas : a valuable digital tool," *Solar Energy*, vol. 71, 2001.
- [17] E. Vartiainen, "A comparison of luminous efficacy models with illuminance and irradiance measurements," *Renewable Energy*, vol. 20, pp. 265-277, 1999.
- [18] O. Walkenhorst, J. Luthier, C. Reinhart, and Timmer J., "Dynamic annual daylight simulations based on one-hour and one-minute means of irradiance data," *Solar Energy*, vol. 72, no. 5, pp. 385-395, 2002.